Development 124, 2691-2700 (1997)
Printed in Great Britain © The Company of Biologists Limited 1997
DEV4884

The PDGFα receptor is required for neural crest cell development and for normal patterning of the somites

Philippe Soriano

Division of Basic Sciences, Fred Hutchinson Cancer Research Center, 1100 Fairview Avenue North, Seattle, WA 98109, USA
(e-mail: psoriano@fhcrc.org)

SUMMARY

Platelet-derived growth factors (PDGFs) have been implicated in the control of cell proliferation, survival and migration. *Patch* mutant mice harbor a deletion including the *PDGFαreceptor* gene and exhibit defects of neural crest origin which affect pigmentation in heterozygotes and cranial bones in homozygotes. To verify the role of the *PDGFαR* gene during development, mice carrying a targeted null mutation were generated. No pigmentation phenotype was observed in heterozygotes. Homozygotes die during embryonic development and exhibit incomplete cephalic closure similar to that observed in a subset of *Patch* mutants. In addition, increased apoptosis was observed on pathways followed by migrating neural crest cells. However, alterations in mutant vertebrae, ribs and sternum were also observed, which appear to stem from a deficiency in myotome formation. These results indicate that PDGFs may exert their functions during early embryogenesis by affecting cell survival and patterning.

Key words: PDGFαR, somite, neural crest, growth factor, mouse, *Patch*, cell proliferation, cell migration, apoptosis

INTRODUCTION

Over the years a number of classical and targeted mutations have been accumulated in the mouse that affect neural crest derivatives or skeletal development (Grüneberg, 1963). Neural crest cells migrate from the dorsal neural tube and give rise to an astounding variety of cell types, including neurons, glia, pigment cells and facial bones (for reviews, see Bronner-Fraser, 1995; Le Douarin et al., 1993). In the trunk, these cells need to migrate around or through blocks of paraxial mesoderm, the somites. In time, somites give rise to sclerotome, myotome and dermatome, the precursors of bones, muscle and dermis, respectively. Genetic studies as well as cell biological evidence have shown that the molecular pathways underlying normal development or proper patterning of these cell types include control of cell proliferation and survival, as well as migration along extracellular matrices or guidance by chemotactic or repulsive cues.

Many growth factors may be involved in controlling these processes. Platelet-derived growth factors (PDGFs) have been shown to regulate not only cell growth and survival, but also various aspects of cell morphology and movement, such as scattering, chemotaxis or deposition of extracellular matrix (for a review, see Claesson-Welsh, 1994; Kazlauskas, 1994). These factors derive their name from their original isolation from platelets and have been shown to have an important role in vascular biology, but they are also known to stimulate the proliferation of many other cell types during development and in the adult (Ross et al., 1986). PDGFs are disulfide-bonded homodimers or heterodimers of two polypeptide chains, A and B. Their receptors are two tyrosine kinases, PDGFαR (αR) and PDGFβR (βR), which can also homodimerize or heterodimerize upon binding of the ligand (Seifert et al., 1989). Previous work has shown that the βR, which binds only PDGF BB with high affinity, is required for normal development of the kidney and the microvasculature (Soriano, 1994), but PDGFR functions earlier in development may be masked by the presence of the αR, which can bind all PDGF isoforms. Further information on the role of PDGF receptors during development has been obtained from studies in *Xenopus* embryos, where the introduction of a dominant negative PDGF receptor leads to abnormal gastrulation (Ataliotis et al., 1995), and mutations in the PI3 kinase binding sites in the receptor lead to abnormal spreading of mesodermal cells (Symes and Mercola, 1996).

A deletion encompassing the *αR* gene, found in *Patch* (*Ph*) mutant mice, has been interpreted as a model of αR deficiency. *Ph* mutant mice, initially studied by Grüneberg and Truslove (1960), exhibit defective melanocyte migration in heterozygotes leading to a white patch in the trunk. The phenotype of the homozygous mutants depends on their genetic background: on a C57BL6/J background, homozygotes die by E10.5 and exhibit multiple defects including reduced growth, dilation of the pericardium, subepidermal blebs, a wavy neural tube and defects in the yolk sac (Orr-Urtreger et al., 1992). However, when backcrossed to CBA or Balb/C background, about a third of the embryos survive until E16-17 and exhibit a cleft face and *spina bifida* (Grüneberg and Truslove, 1960; Schatteman et al., 1992). The cleft face phenotype has been associated with a defect in the migration of cranial neural crest cells (Morrison-Graham et al., 1992), although it remains unclear if this defect

is on their migration pathway or associated with the neural crest cells themselves.

The Ph mutation, however, represents a large deletion that involves more than one gene and for which both breakpoints have not been mapped (Brunkow et al., 1995; Nagle et al., 1994; Smith et al., 1991; Stephenson et al., 1991). In particular, the deletion extends towards, but does not include, the neighboring *c-kit* gene, which is involved in migration of a number of different cell types including melanocytes. Moreover, the domain of expression of *kit* is altered in Ph heterozygotes (Duttlinger et al., 1995; Wehrle-Haller et al., 1996), raising the possibility that this may be responsible for the pigmentation defect. In this work, I have generated mice carrying targeted mutations in the *PDGFαR* gene and discuss the mutant phenotypes in comparison with Ph and in light of roles that this receptor may play in cell survival during development.

MATERIALS AND METHODS

Derivation of mutant mice

The *PDGFαR* locus was isolated from a 129Sv genomic library using a full-length αR cDNA plasmid (provided by Dan Bowen-Pope and Chuck Stiles). The targeting construct used to derive the αR1 strain was constructed using a neo expression cassette (PGKneobpA; Soriano et al., 1991) to replace a 0.5 kb *Eco*RI-*Spe*I genomic fragment encompassing part of the first immunoglobulin domain, flanked by 7 kb (*Sac*II-*Eco*RI) and 1.1 kb (*Spe*I-*Xba*I) genomic sequences derived from a 129Sv library. The targeting construct used to derive the αR2-4 strains was constructed in PGKneolox2DTA, a plasmid containing a *neo* gene flanked by lox sites, a negative selection cassette (PGK-DTAbpA) and polylinker sites for the insertion of flanking sequences. This targeting vector replaces a 6.5 kb *Bam*HI-*Sma*I fragment (corresponding to the signal peptide, first and second immunoglobulin domain) with the neo cassette and includes 5.2 kb (*Sac*II-*Bam*HI) and 2.7 kb (*Sma*I-*Eco*RV) of 5′ and 3′ sequences, respectively. The constructs were linearized, electroporated into 129Sv-derived AK7 ES cells (A. Imamoto and P. S., unpublished data), and colonies were selected with G418. Homologous recombination events were screened by PCR as described (Soriano et al., 1991), using primers from the *neo* gene and genomic sequences outside of the targeting construct. Southern blots were done using αR cDNA probes (*Eco*RI-*Pst*I 614 bp fragment for the αR1 strain; *Eco*RV-*Nco*I 239 bp fragment for the αR2-4 strains). The blots were rehybridized with neo to show that there was only a single insertion of the vector and with plasmid to verify the absence of a concatemer. Tissue culture and blastocyst injections were as described previously (Soriano et al., 1991). Southern, northern and western blots were done according to standard procedures. No upregulation of βR expression level was observed on whole embryo extracts using antibodies specific to the βR (provided by Andrius Kazlauskas).

PCR genotyping was performed on tail biopsies or yolk sac DNAs as described (Imamoto and Soriano, 1993) using the following combination of primers for the αR1 strain: 5′-TCA TCT CCT GCC AGC TCT TAT TAC-3′, 5′-TCC GTC TGA GTG TGG TTG TAG TAG-3′, and 5′-TCT GAG CCC AGA AAG CGA AG-3′. This produces 265 and 420 bp diagnostic fragments for the wild-type and mutant allele, respectively. αR2-4 embryos were genotyped using the following primers: 5′-CCC TTG TGG TCA TGC CAA AC-3′, 5′-GCT TTT GCC TCC ATT ACA CTG G-3′ and 5′-ACG AAG TTA TTA GGT CCC TCG AC-3′. This reaction produces 451 bp and 242 bp fragments for the wild-type and mutant alleles, respectively.

Histological and skeletal analysis

The day the vaginal plug was observed was considered as embryonic day 0 (E0). Embryos were fixed in 4% paraformaldehyde or Bouin's, embedded in paraffin, sectioned at 6 μm and stained with hematoxylin and eosin, or methyl green. For skeletal preparations, embryos were fixed in 95% ethanol, stained at 37°C in 0.015% alcian blue, 0.005% alizarin red, 5% acetic acid in 70% ethanol, cleared in 0.5-1% KOH and transferred to solutions of decreasing KOH strength and increasing glycerol concentration.

Whole-mount in situ procedures

Whole-mount in situ hybridizations and immunohistochemistry were performed essentially as described (Hogan et al., 1994). The following probes were used for in situ hybridization: myogenin (from Norbert Kraut), myoD (antisense probe from nucleotide 1781 to nucleotide 751, from Atsushi Asakura); Pax1 (Pax1 HIS, from Rudi Balling), twist (from Bill Shawlot and Richard Behringer), and TRP-2 (from Berni Wehrle-Haller). Monoclonal antibodies were obtained from Atsushi Asakura and Steve Tapscott (myosin heavy chain, MF-20), Tom Jessell (neurofilament, 2H3), and Pharmingen (CD31/PECAM-1) and polyclonal antibodies were provided by Andrius Kazlauskas (27P and 29P, PDGFαR; 30A, PDGFβR) and Albert Candia and Chris Wright (Mox-1). Proliferating cells were detected in sections of embryos labelled for 1 hour by injection of pregnant females with 100 μg BrdU/g body weight, using a monoclonal antibody to BrdU (Becton Dickinson) and a Vectastain Elite ABC kit (Vector Laboratories, Burlingame, CA). The 'whole death' (TUNEL) procedure (Conlon et al., 1995) was used to examine apoptosis in E9-E10 embryos.

RESULTS

Derivation of mutant mice

Two different mutations were introduced into the *αR* gene (Fig. 1A). The first targeting vector (α6) generates a small (~0.5 kb) deletion corresponding to the first immunoglobulin (Ig) domain. A second targeting construct (α16) carries a larger deletion (~6.5 kb) corresponding to the signal peptide, as well as the first and second Ig domains. Following electroporation into ES cells, 7/56 (α6) and 18/384 (α16) G418^r clones identified by PCR had undergone homologous recombination and were subsequently verified by Southern blot analysis (Fig. 1B). One clone derived from an α6 targeting event and three clones derived from α16 targeting events were used to derive germline chimeras and gave rise to the *αR1* and *αR2-4* mutant strains, respectively. Heterozygous offspring had normal agouti pigmentation and did not display the white patch observed on the trunk of *Ph* mice. Moreover, no defect in the migration of melanocytes could be detected in E10-E13 homozygous embryos by in situ hybridization, using a TRP2 (tyrosinase related-protein 2) probe as a marker of melanocytes (Fig. 2).

Although heterozygous mice did not display a pigmentation phenotype, chimeric mice derived from the heterozygous αR ES cells gave very poor coat color chimerism (ranging from not detectable to 30% at the most), whereas chimeras made in parallel with ES cell clones in which the αR locus was not targeted, or in which the αR locus was targeted with a conditional mutation that does not eliminate αR expression (unpublished data), produced extensive (50-100%) coat color chimerism. Tail biopsies revealed extensive (over 50%) contribution of the mutant cells and test breeding of seven chimeras representing four targeted clones demonstrated in each case germ-line transmission of the mutant allele in the first litter, with progeny from six of the seven chimeras exclusively

derived from the injected ES cells. These results suggest a dosage-sensitive, cell autonomous phenotype of the mutation on coat color pigmentation.

Heterozygous offspring were mated to derive homozygous embryos. Protein lysates from homozygotes were subjected to western blot analysis using antibodies directed against the kinase domain or the carboxy terminus of the αR. In lysates of *αR1* mutant embryos, a weak low molecular weight band, migrating at about 140×10^3 M_r (Fig. 1C), was observed. Northern blot analysis suggests that this truncated protein might be due to splicing from an exon encoding the signal peptide to an exon corresponding to the second immunoglobulin domain (not shown), which would not lead to a frameshift mutation (Wang and Stiles, 1994). A similar mutation, tested in fibroblasts, led to the formation of a receptor that was not glycosylated, did not go to the cell surface and thus did not bind the ligand (Yu et al., 1994). In contrast, western blot analysis of lysates from E12 αR2-4 embryos, using several antibodies raised against different parts of the receptor, failed to reveal any immunoreactive bands (Fig. 1C), indicating that the larger deletion leads to a null allele. Identical phenotypes were observed with both mutations indicating that the truncated molecule in the αR1 strain is unlikely to be of any physiological consequences. In addition, the similarity of the phenotype observed with both mutations argue against any effect that may have been imparted by the neo cassette or the location or size of the deletion.

Lethality of homozygous mutant embryos

No homozygous mutant mice were recovered from double heterozygous crosses. Timed pregnancies therefore were examined between E8 and E16 of gestation (Table 1). Close to expected numbers of homozygous embryos were recovered at various stages, on a congenic 129Sv or mixed 129Sv × C57BL/6J genetic backgrounds, as well as after four-generation backcross to C57BL/6J, but many embryos exhibited severe developmental defects. At E8, five out of six embryos had a very wavy neural tube and had not turned, one was severely retarded (headfold stage) and two had 2-4 subepidermal blebs flanking the neural tube (Fig. 3A). At E9, almost all of the embryos still displayed a wavy neural tube, and 25% of these were smaller and had not turned about their anterior-posterior axis. A few of these embryos also exhibited blebs filled with blood along the neural tube as well as on the head (Fig. 3B), or a dilated pericardium and defective yolk sac vasculature. At E10, more than half of the embryos had a very wavy neural tube, one quarter had a dilated pericardium and one quarter were very small; three embryos had not turned about their anterior-posterior axis and four exhibited subepidermal blebs. However, almost one quarter of the mutant embryos at E10 appeared normal, relative to wild-type or heterozygous embryos. At E11, more than half of the embryos were normal and the others were smaller and displayed a wavy neural tube.

Table 1. Genotype of PDGFaR null mutant embryos

	+/+	+/–	–/–
E8	1	11	6 (33%)
E9	18	33	18 (26%)
E10	68	147	65 (23%)
E11	9	16	7 (22%)
E12	9	16	3 (11%)
E13	23	33	9 (14%)
E14	16	26	9 (18%; 3 dead)
E15	20	37	19 (25%; 11 dead)
E16	19	30	6 (11%; 4 dead)

At E12 and later, the mutant phenotype was less variable and embryos displayed large blebs on their heads accompanied by a cleft (Fig. 3C,D). The embryos also displayed blebbing in multiple locations and oedema, which increased in severity by E13, but all of the embryos were still alive. At E14, several mutant embryos were dead and survivors were distended and exhibited bleeding at various locations. Most of the embryos

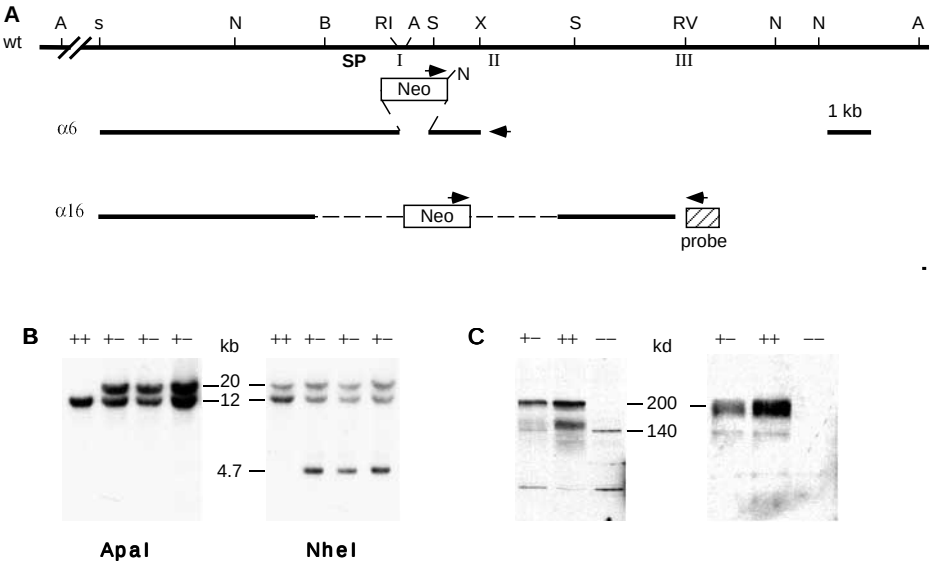

Fig. 1. Targeted disruption of the *PDGFαR* gene. (A) Map of the genomic locus. The α6 and α16 targeting vectors, used to derive the αR1 and αR2-4 strains, respectively, are shown. Arrowheads mark the position of PCR primers used to detect targeted insertions. The neo cassette (neo) in α16 is flanked with *loxP* sites for Cre recombinase. A, *Apa*I; s, *Sac*II; N, *Nhe*I; B, *Bam*HI; RI, *Eco*RI; S, *Sma*I; X, *Xba*I; RV, *Eco*RV. Not all restriction sites are shown. SP, I, II and III represent the approximate positions of cDNA sequences encoding the signal peptide, first, second and third immunoglobulin domain, respectively. (B) Southern blot analysis of wild-type (++) and targeted α16 (+–) ES cell DNAs digested with *Apa*I or *Nhe*I. *Apa*I does not cut in the targeting vector, and the 20 kb fragment is diagnostic for normal integration of the vector on the 5′ side. The probe used to detect α16 targeted events (hatched box in A) is derived from the αR cDNA, and also hybridizes further 3′ to *Nhe*I fragments of 1 kb (not shown) and 20 kb. (C) Western blot analysis of whole E10 αR1 (left) and E12 αR4 (right) embryos, using a polyclonal antibody (27P) to the αR. ++, wild type; +–, heterozygotes; – –, homozygotes. Note the presence of a 140×10^3 M_r fragment in lysates from heterozygous and homozygous αR1 embryos. The diffuse band of higher mobility in wild-type lysates represents the non-glycosylated form of the receptor.

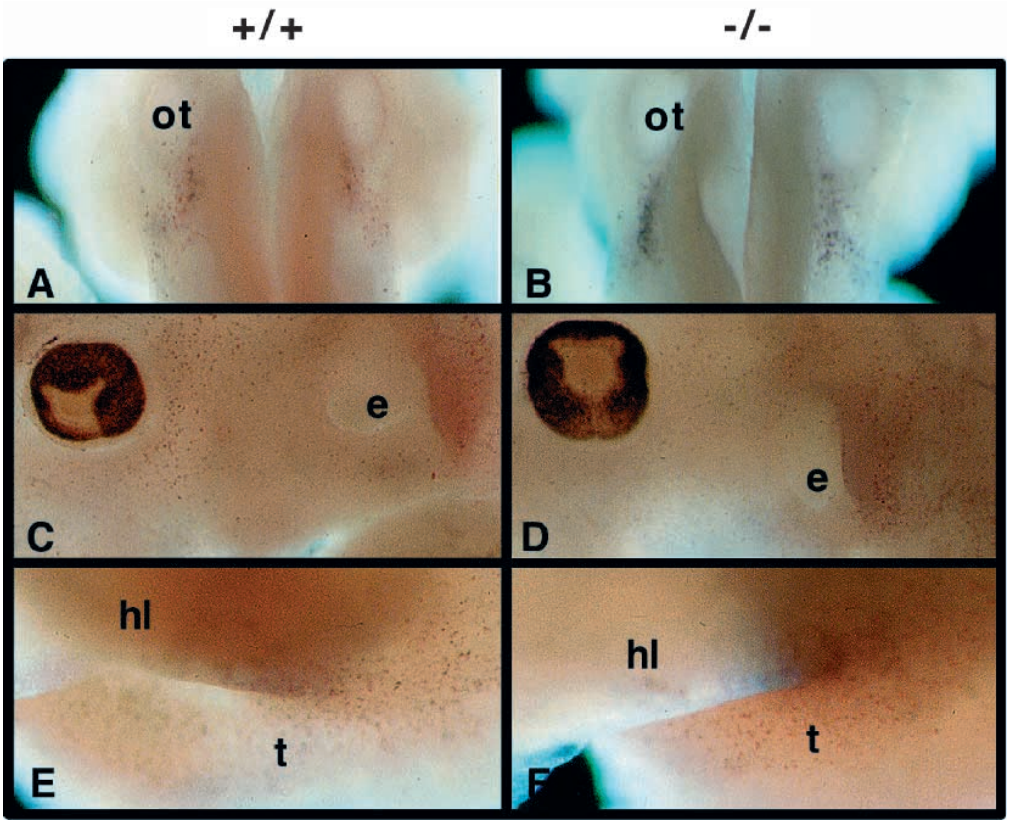

Fig. 2. Normal melanocyte development in mutant embryos. (A,B) E.10.5. Melanocyte precursors, visualized by hybridization with TRP-2, can be identified as a stream of cells migrating, caudally from the otic vesicle (ot). (C,D) E13.5. Lateral views at the level of the eye and ear (e). (E,F) E13.5. Lateral views at the level of the tail (t) and hindlimb (hl). Note the normal number of melanocytes around the ear and tail, which are lacking in Patch mutant embryos (Wehrle-Haller et al., 1996).

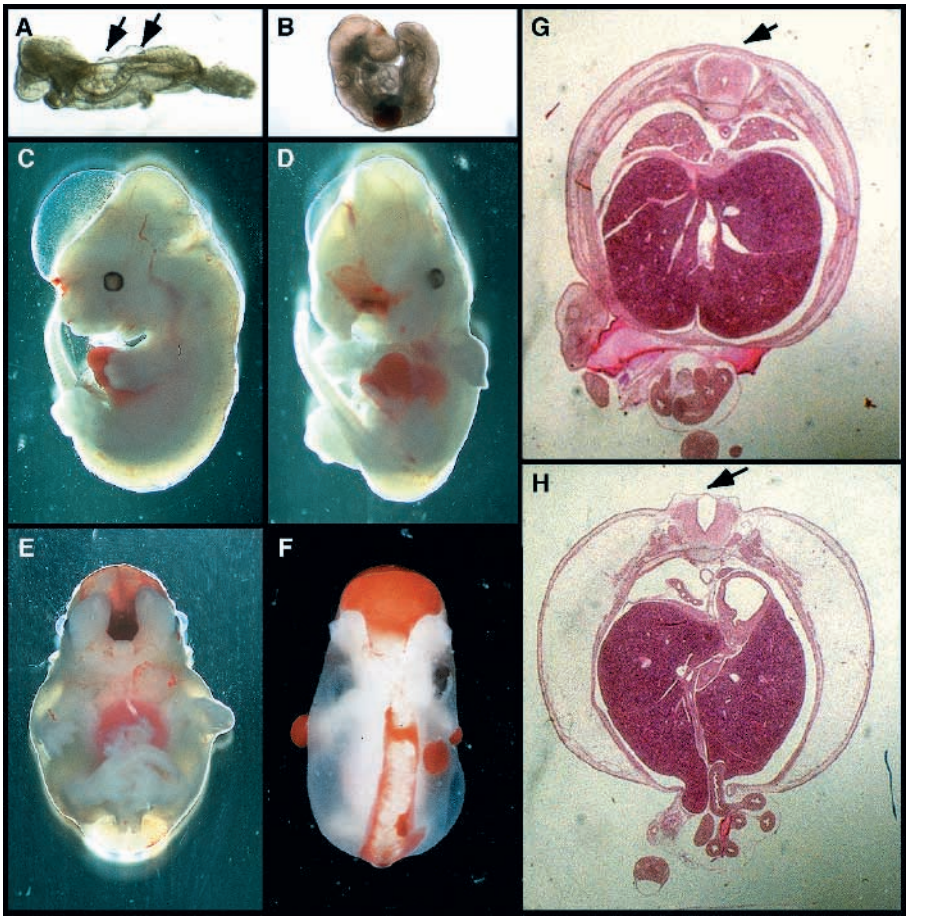

Fig. 3. Phenotypic abnormalities in mutant embryos. (A) E 8.5. The arrows indicate subepidermal blebs flanking the neural tube. (B), E9.5. Note a bleb filled with blood. (C,D) E12.5 embryo, showing a large bleb on the head accompanied by bleeding and a cleft face. (E,F) E15.5 embryos, exhibiting significant oedema, bleeding, and a cleft face. (G,H), cross section through a wild-type (G) and mutant (H) E15.5 embryo. Note oedema, abnormal dorsal neural tube and bulging out of the liver.

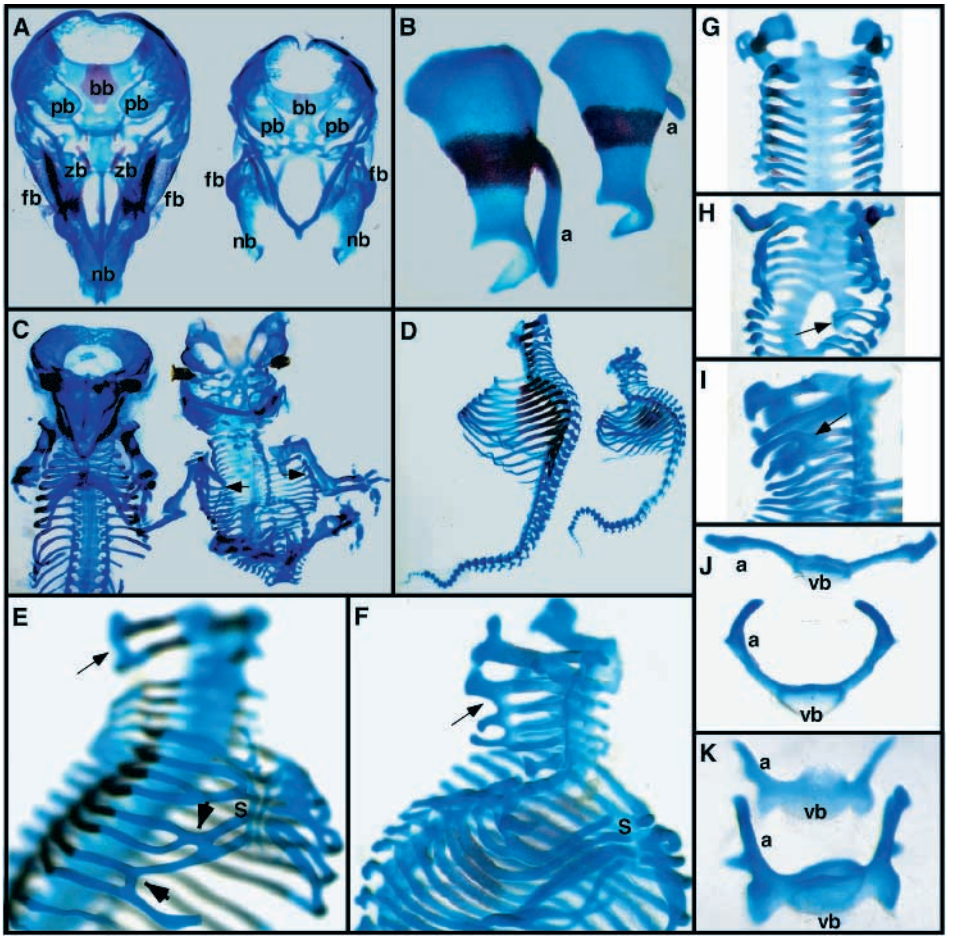

Fig. 4. Skeletal abnormalities in mutant E15.5 embryos. (A) Cranial bones. wt, left; mutant, right. bb, basisphenoid bone; pb, parietal bone; fb, frontal bone; zb, zygomatic bone; nb, nasal bone. Note the failure in the mutant for the nb to fuse, and retardation or absence of other bone structures. (B) Scapula. wt, left; mutant, right. Note the poor development of the acromion (a). (C) Thoracic cavity. wt, left; mutant, right. Note the failure for the sternal bands (arrows) to meet in the mutant. (D) Side view of spinal column. wt, left; mutant, right. Note the severe arching in the mutant. (E,F) Rib fusions in mutant embryo (heavy arrowheads) and incomplete fusion of the sternal bands. s, sternal bands. (G-I) Frontal view of cervical vertebrae from wt (G) and mutant (H-I) embryos. Note different levels of vertebral fusions (arrows; also in E and F)). (J) Dissected ninth thoracic vertebrae from wt (bottom) and mutant (top) embryos. Note the absence of flexure of the mutant vertebra. a, vertebral arch; vb, vertebral body. (K) Dissected first sacral vertebrae from wt (bottom) and mutant (top) embryos.

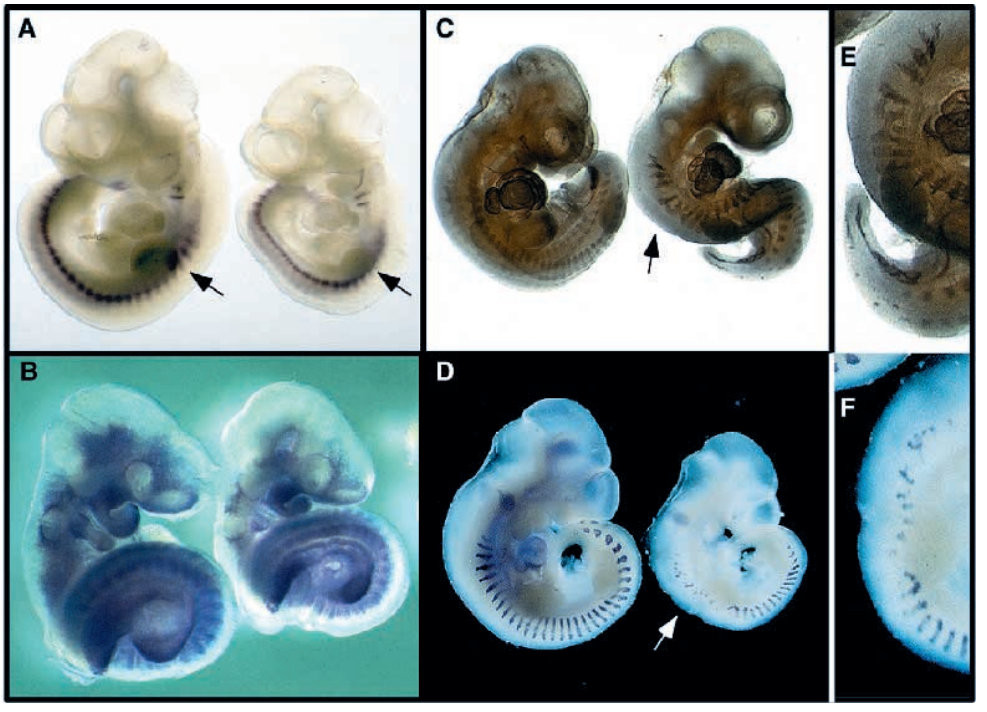

Fig. 5. Expression of sclerotome (A,B) and myotome (C-F) markers in wild-type (leftmost) and mutant E10.5 embryos. (A) Pax1 in situ hybridization. This marker is expressed normally in mutant somites, but is absent from the anterior proximal limb bud. (B) Twist is expressed normally in mutant embryos as seen by in situ hybridization. (C) Whole-mount immunohistochemistry for myosin heavy chain expression, detected following partial clearing of the embryos. Note in wild-type embryo the absence of a ventral myotome in the most rostral somites and the rounded shape of the myotome. The myotome in the rostral somites of the mutant embryo (arrow) has an elongated shape, is missing in the fifth most rostral somite and is fused between the seventh and eighth somite. (D) Dark-field photomicrograph of myogenin in situ hybridization. Note the alterations in myogenin expression in the most rostral somites (arrow) of the myotome. The abnormalities seen in C and D in the rostral myotome of mutant embryos are enlarged in E and F, respectively.

were dead by E16, but survivors exhibited accentuated phenotypes, with extensive bleeding in the head and along the vertebral column, which appeared enlarged (Fig. 3E,F). The extensive hemorrhaging observed in the mutant embryos is a likely cause of death.

Histological sections through mutant embryos confirmed the extensive oedema (Fig. 3G,H). The skin was distended, and the epidermal layer was very thin and separated from any dermal layer when blebbed, perhaps similar to the phenotype observed in Ph embryos (Schatteman et al., 1992). The neural tube was abnormally thin dorsally and lacked a roof plate (arrow in Fig. 3H). Moreover, tissues such as liver were bulging from the abdominal wall musculature. Despite the extensive bleeding in the mutants, a thinning of the vasculature or cardiac defects were not immediately apparent in tissue sections or following whole-mount immunohistochemistry for PECAM-1 (Baldwin et al., 1994) and septation in the heart had proceeded normally in at least some of the surviving E15 embryos.

Skeletal abnormalities in mutant embryos

Skeletal preparation were made from E13-E15 embryos. This examination revealed significant defects in the skull, most conspicuous in the anterior bones (Fig. 4A). In particular, the nasal bone failed to fuse in the midline. The frontal bone and, to a lesser extent, the parietal bone exhibited incomplete fusion towards the top of the skull. The zygomatic bone, which was partially ossified by E15 in wild-type embryos, was undetectable in the mutants. The basisphenoid and temporal bones were retarded, whereas the basiooccipital bone and the maxilla appeared grossly normal.

Skeletal abnormalities were also detected in the acromion of the scapula (Fig. 4B) and in the vertebral column and the rib cavity (Fig. 4C,D). Normal numbers of ribs were observed and all of these were attached to the vertebrae. Almost all embryos exhibited varying degrees of rib fusions or bifurcations, but these were not symmetric on both sides of the sternum (Fig. 4E,F). These defects were already observed at E13, when chondrification is first evident (not shown). Most of the ribs were attached to the sternal bands. The sternal bands however were shorter than in wild-type embryos, very irregular and failed to fuse. Another abnormality in the vertebral column was with the vertebrae themselves. In particular, the cervical vertebrae showed extensive structural alterations and anterior-posterior fusions of the arches, in some instances involving as many as four cervical vertebrae (Fig. 4E-I). Moreover, the apposition of the vertebrae at the level of the vertebral bodies was abnormal and bilaterally asymmetric. In thoracic vertebrae, and to a lesser extent cervical vertebrae, the neural arches failed to form the convex structure observed in wild-type embryos, resulting in *spina bifida* (Fig. 4J) and in an abnormal curvature of the spinal column (see Fig. 4D). However, besides slightly delayed development, sacral and caudal vertebrae appeared normal (Fig. 4K).

Somitic differentiation affects the myotome

To investigate further the mechanisms underlying the observed phenotypic abnormalities, the expression of a number of markers of somite differentiation were examined in whole embryos. Somites bud off from the rostral end of the paraxial mesoderm and, as they develop, cells become specified to form the sclerotome, which occupies a ventral position, and the dermomyotome on the dorsal side. The sclerotome will eventually form bone, while the dermomyotome generates the dermatome and later the dorsal skin, and the myotome, which forms muscle. The pattern of expression of *PDGFαR* and *PDGFA* during development has been extensively analyzed (Orr-Urtreger and Lonai, 1992), with the receptor initially expressed throughout the undifferentiated somite and later restricted to the sclerotome and to a lesser extent the dermatome, while *PDGFA* is expressed in the myotome. Whole-mount immunohistochemistry using a polyclonal antibody to Mox1, a relatively late marker of paraxial mesoderm, which labels the whole somite (Candia et al., 1992), failed to reveal any reproducible defects in the mutant embryos, except for the fact that smaller embryos had correspondingly smaller somitic condensations (not shown). To identify potential defects in more detail, embryos were probed with two markers that label the sclerotome, Pax1 and Twist. Again, no difference in the expression of these genes was observed in the sclerotome (Fig. 5A,B), despite the fact that *undulated* mutant mice, which carry a mutation in the *Pax1* gene (Balling et al., 1988), have been shown to interact genetically with *Patch* mice, leading to *spina bifida* (Helwig et al., 1995). However, *Pax1* is expressed in the anterior proximal part of the forelimb bud, and this expression was significantly reduced in several mutant embryos, which may lead to the defect in the acromion of the scapula (Fig. 4B). Interestingly, *undulated* mice exhibit a similar skeletal defect (Grüneberg, 1963).

One of the defects observed in the mutant embryos affects the ribs. Ribs have been shown to be significantly reduced in embryos homozygous for a targeted mutation in the myogenic factors *myf5* (Braun et al., 1992), or fused in embryos carrying some mutant alleles of the *MRF4/myf6* gene (for a review, see Olson et al., 1996). Expression of both of these factors is restricted to the myotome. To examine a potential defect in the myotome, mutant embryos were probed for the expression of myosin heavy chain protein. This analysis revealed significant disorganization, especially at the level of the more rostral somites. Instead of adopting the round shape observed in wild-type embryos, mutant myotomes were elongated, missing or fused with adjacent myotomes (Fig. 5C,E). The altered appearance of the myotome, using this marker, was confined to the 15-20 most rostral somites at E10.5, while myotomal structure appeared normal in caudal somites. These observations were extended using whole-mount hybridization with probes to myogenin and MyoD. Consistent with the above results, hybridization with the myogenin probe revealed defects in the rostral somites (Fig. 5D,F). However, such defects were less obvious with MyoD (not shown), as this probe labels preferentially the ventral myotome that is normally lacking in rostral somites (see for instance Fig. 5C). Taken together, these results suggest that the neural tube defects seen in early mutants and the vertebral and rib abnormalities observed later in development may be secondary to a deficiency in myotome patterning.

Cell proliferation and cell death in mutant embryos

PDGFs were initially identified as mitogenic growth factors but have also been shown to act as survival factors. It is possible therefore that the defects observed in the mutant embryos might be due to abnormal cell proliferation, cell death, or both. To further examine these possibilities, embryos were labeled with 5-bromodeoxyuridine (BrdU) to identify cells in S-phase of the cell cycle. No obvious reduction in proliferation was

observed by counting labeled cells in tissue sections either at E10 or E14 (not shown). However, some tissues or cell types may be affected that were not detected. In particular, although labeling was observed throughout various bones, the shorter length of the arches in thoracic vertebrae, and the ensuing *spina bifida*, might be indicative of reduced cell proliferation.

Apoptotic cell death was examined at E9 and E10 by the 'whole death' procedure (Conlon et al., 1995). No significant difference between wild-type and mutant embryos was observed at E9; however, by E10, increased apoptosis in mutant embryos compared to wild type was observed in the somites, as well as in the cephalic region and the branchial arches (Fig. 6A). Sections through the labeled embryos revealed the presence of some apoptotic cells in the trunk close to the roof plate of the neural tube and within the sclerotome, reflecting the migratory pathways adopted by neural crest cells where normal cell death has been observed (Jeffs and Osmond, 1992). However, the clearest labeling was in the dermomyotome (Fig. 6B,C). Although the absolute number of apoptotic nuclei varied from experiment to experiment, there was a consistent increase in cell death in mutants in four separate experiments. The average number of apoptotic cells per somite (sectioned through rump of embryo) was 8.03±3.31 s.d. in the mutant shown in Fig. 6C (n=35 sections) versus 3.22±2.58 s.d. in a wild-type littermate (not shown). In the cranial areas, increased cell death was observed in a stream of cells flanking the otic vesicle as well as in the branchial arches (Fig. 6D-G). Again, this corresponds to the area of migration of neural crest cells (Jeffs et al., 1992). Importantly, the observed defects in the heads of the mutant embryos are consistent with the absence of neural crest cell derivatives (Morrison-Graham et al., 1992). Despite extensive cell death in this region, neuronal derivatives of cranial neural crest cells appeared to migrate properly, as observed by neurofilament expression (data not shown). These results suggest that the defects observed in *PDGFαR* mutant embryos might be due in part to increased apoptosis of a non-neuronal subset of cranial neural crest cells.

DISCUSSION

Two different mutations targeted into the *PDGFαR* gene indicate a requirement for PDGF signaling in cranial neural crest development and in the normal patterning of the somites. Several aspects of the mutant phenotype reported here differ from that observed for Ph mice, which harbor a deletion of the *αR* gene (Table 2). The first and most conspicuous difference is the absence of a pigmentation defect in heterozygotes. The close linkage between the *Ph* and *W* mutations, originally observed by Grüneberg and Truslove (1960), and the subsequent identification of the *kit* receptor tyrosine kinase gene at the W locus (Chabot et al., 1988; Geissler et al., 1988), have led to long-standing speculations that the pigmentation defect in Ph might be somehow related to *kit* misexpression. In support of this possibility, Ph heterozygous embryos exhibit an enlarged domain of expression of *kit* in the somites (Duttlinger et al., 1995; Wehrle-Haller et al., 1996). However, the lack of a pigmentation defect in *αR* mutants does not prove that altered *kit* expression is responsible for that phenotype in Ph, but merely that the αR is not absolutely required for melanocyte migration.

Table 2. Summary of *PDGFαR* and *Ph* mutant phenotypes

	PDGFαR	Ph
Survival on C57BL6/J	Up to E16 (N4 backcross)	up to E10
Trunk crest	No pigmentation defect	Pigmentation defect (+/–, –/–)
Cardiac crest	Septation	No septation
Cranial crest	Cleft face	Cleft face
Skeleton	Spina bifida	Spina bifida
	Fusions of cervical vertebrae and ribs; truncated acromion	Not reported

αR mutants differed from Ph by several features other than the absence of a melanocyte migration defect. First, approximately 80% of the mutant embryos survived up to E13 following six backcross generations to C57BL/6J, whereas less than 3% of Ph embryos survive on the same background (Orr-Urtreger et al., 1992); and data not shown). In addition, many *αR* mutant embryos were recovered up to E16, even if they were often dead, whereas only one third of *Ph* mutant embryos made it to this stage when backcrossed onto CBA (Grüneberg and Truslove, 1960) or Balb/c (Schatteman et al., 1992) backgrounds. However, embryos homozygous for the 'Patch extended' mutation (an even larger deletion) occasionally survive to birth (Truslove, 1977). Taken together, these observations indicate the presence of modifier loci linked to the *αR* gene, which affect embryo survival in various mutant backgrounds. Second, although fusions of the cervical vertebrae, ribs and the defects in the sternum have recently been reported in *Ph* in addition to the cleft face and *spina bifida* phenotypes, some *Ph* embryos carry an extra rib (Payne et al., 1997). Third, *Ph* embryos exhibit a frequent defect in septum formation in the heart (Morrison-Graham et al., 1992), whereas this process appears to proceed normally in at least some *αR* mutants examined at E15. These results indicate that the *Ph* phenotype is multigenic, with some but not all features attributable to the loss of the PDGFαR.

The skeletal defects observed in the trunk are complex and include fusions of the cervical vertebrae and of the ribs, altered flexure of the thoracic vertebrae and incomplete development of the sternum. All of these bones derive from the sclerotome, which expresses the αR, whereas PDGF A is expressed in the myotome (Orr-Urtreger et al., 1992; Orr-Urtreger and Lonai, 1992). Based on these expression patterns, the observed defects might be expected to stem from an initial deficiency in the sclerotome. However, the alternate expression of the ligand and receptor in the myotome and sclerotome might indicate a signaling pathway between the two compartments required for normal sclerotome development. Surprisingly, myotome but not sclerotome markers were the ones to highlight deficiencies in the somites. At a gross level, however, muscle formation appeared normal in later stage embryos. The alterations in patterning were especially noticeable in the more rostral somites, which either showed an absence of myotome, myotomal fusions between somites or an elongated shape of the myotomal compartment. This result might indicate different requirements for growth factors or different growth factor expression patterns along the rostral-caudal axis.

A number of classical and targeted mutations have been shown to lead to deficiencies in rib formation, but those in the myogenic genes reinforce the importance of myotome-to-

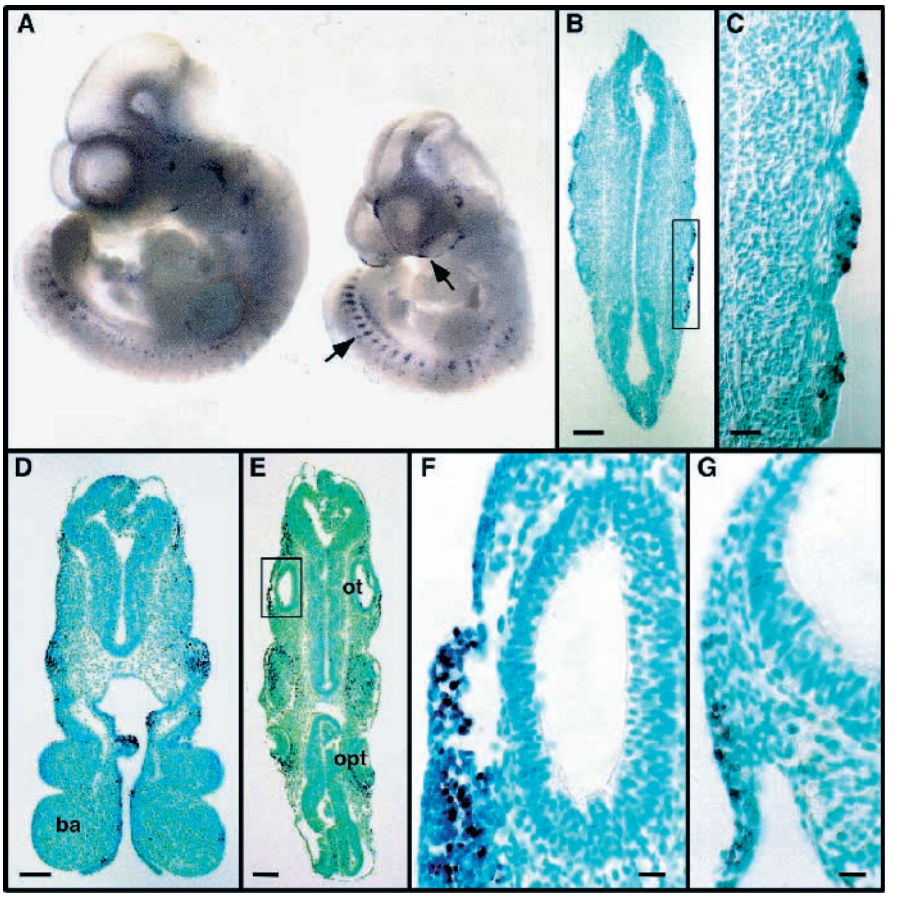

Fig. 6. Apoptotic cell death in wt and mutant E10.5 embryos, as detected by the 'whole death' method. (A) Whole-mount labeling of apoptotic cells in wt (left) and mutant (right) embryos; note the increased apoptosis in the mutant at the level of the somites and in some areas of the head (arrows). (B-G) Cross sections of mutant (B-F) and wt (G) embryos counterstained with methyl green. (B) Transverse section through the rump of a mutant embryo, bar 100 μm; note the presence of apoptotic cells just between the surface ectoderm and the myotome. (C) Higher magnification of box shown in B, Nomarski optics, bar 25 μm. (D) Cross section at the level of branchial arches (ba); bar 100 μm. (E) Cross section through the head; bar, 100 μm. Apoptotic cells are observed at the level of the optic (opt) and otic (ot) vesicles. (F) Higher magnification of box shown in E; bar 16 μm. (G) Cross section through an equivalent section of the otic vesicle in a wild-type littermate; bar 16 μm. Although apoptotic cells are visible anteriorly, there are far fewer than in F.

sclerotome signaling. In the case of the *MRF4/myf6* gene, the variability in the rib fusion phenotype between different mutant strains has been attributed to position effect interference of the neo targeting cassette (for a review, see Olson et al., 1996) with the expression of the neighboring *myf5* gene, which is required for rib formation (Braun et al., 1992). Interestingly, the *myf5* mutation eliminates FGF4 and FGF6 expression in the myotome, and members of the FGF and TGFβ family are able to stimulate chondrogenesis in somite micromass cultures (Grass et al., 1996), as does PDGFA (M. Tallquist and P.S., unpublished data). These results suggest that multiple growth factors may be involved in myotome-to-sclerotome signaling. Although the αR may act autonomously in the myotome if it is expressed there at low levels, its earlier expression in the undifferentiated somites rather suggests a defect in the initial formation of the myotome. It is also possible that the defect in myotome formation arises from a feedback mechanism from the sclerotome, due to the absence of the αR. Last, subepidermal blebs might lead to poor contact between the surface ectoderm and the neural tube or undifferentiated somites, and be a contributing factor preventing proper dorsalization of the neural tube and the formation of myotome (Fan and Tessier-Lavigne, 1994; Spence et al., 1996) as well as neural crest cells (Dickinson et al., 1995; Liem et al., 1995; Selleck and Bronner-Fraser, 1995).

In the head, the observed defects were similar if not identical to those observed for Ph embryos and have been attributed to a failure of a subset of non-neuronal neural crest cells, which exhibit high levels of αR expression, to migrate to their proper destinations (Morrison-Graham et al., 1992). PDGFs are known to be involved in chemoattraction, and it is possible that such a migratory mechanism may play a role in the mutant phenotype. Conversely, the PDGFαR has also been associated with inhibition of chemotaxis mediated by other growth factors receptors, in particular the βR (Koyama et al., 1992). Alternatively, it has been suggested that the defect in neural crest cell migration in Ph mice might be associated with an alteration in the deposition of the extracellular matrix along the cell migration pathway (Morrison-Graham et al., 1992), as PDGFs are known to be involved in ECM production.

PDGFs were initially identified as mitogens for a number of different cell types, but BrdU incorporation studies in the mutant embryos failed to detect any general decrease in cell proliferation. A more extreme view of potential roles of growth factors has been advanced by Raff and colleagues (Raff, 1992; Raff et al., 1993). According to this viewpoint, cells would normally undergo cell death if not sustained by growth factors. A role of PDGF as a survival factor is substantiated by studies of a number of cell types in culture, including oligodendrocytes (Barres et al., 1992); however, such a role in vivo might be more difficult to demonstrate and there is no direct evidence supporting a direct role for PDGF as a survival factor for neural crest cells. Increased apoptosis was noticed along the pathway of migration of cranial neural crest cells, which express high levels of the αR (M. Bronner-Fraser, personal communication). In vitro cultures of neural crest cells, grafting experiments and

the derivation of mice carrying conditional or point mutations in the receptors may help further understand the cell autonomy and the mechanistic basis for the mutant phenotype.

The genes encoding both PDGF receptors and both PDGF ligands have now been disrupted. βR (Soriano, 1994) and PDGF B mutant embryos (Levéen et al., 1994) exhibit a generally similar phenotype, characterized by hematological and kidney defects. However, the phenotype of PDGF A mutant mice appears to vary significantly from that of the *αR* mutants presented here. Only a small percentage of the PDGF A mice survive past birth, where they exhibit a lung emphysema-like phenotype; and the embryos that die during development do not exhibit the skeletal abnormalities characteristic for the αR mutation (Boström et al., 1996; M. Hellström, C. Betsholtz, and P.S., unpublished observations). Analysis of double receptor and double ligand mutants is underway, which may help further understand the requirements for PDGF during embryogenesis.

This work is dedicated to the memory of Hal Weintraub. I thank Chris Auger for careful and dedicated help with genotyping of mutant mice and embryos; Kari Lindstrum for care of the animals; Brigid Hogan, Peter Rigby and Steve Tapscott for discussions; Dan Bowen-Pope and Chuck Stiles for plasmids; Albert Candia, Tom Jessell, Andrius Kazlauskas, Steve Tapscott and Chris Wright for antibodies; Atsushi Asakura, Rudi Balling, Richard Behringer, Norbert Kraut, Bill Shawlot and Berni Wehrle-Haller for in situ probes; and Marianne Bronner-Fraser, Jon Cooper, Norbert Kraut, Steve Tapscott and my laboratory colleagues for critical reading of the manuscript. This work was supported by grants from the National Institute of Child Health and Human Development and the Markey Molecular Medicine Center.

REFERENCES

Ataliotis, P., Symes, K., Chou, M. M., Ho, L. and Mercola, M. (1995). PDGF signalling is required for gastrulation of *Xenopus laevis*. *Development* **121,** 3099-3110.

Baldwin, H. S., Shen, H. M., Yan, H. C., DeLisser, H. M., Chung, A., Mickanin, C., Trask, T., Kirschbaum, N. E., Newman, P. J., Albelda, S. M. and Buck, C. A. (1994). Platelet endothelial cell adhesion molecule-1 (PECAM-1/CD31): alternatively spliced, functionally distinct isoforms expressed during mammalian cardiovascular development. *Development* **120,** 2539-2553.

Balling, R., Deutsch, U. and Gruss, P. (1988). *Undulated*, a mutation affecting the development of the mouse skeleton, has a point mutation in the paired box of *Pax1*. *Cell* **55,** 531-535.

Barres, B. A., Hart, I. K., Coles, H. S. R., Burne, J. F., Voyvodic, J. T., Richardson, W. D. and Raff, M. C. (1992). Cell death and control of cell survival in the oligodendrocyte lineage. *Cell* **70,** 31-46.

Boström, H., Willetts, K., Pekny, M., Levéen, P., Lindahl, P., Hedstrand, H., Pekna, M., Hellström, M., Gebre-Mehdin, S., Schalling, M., Nillson, M., Kurland, S., Törnell, J., Heath, J. K. and Betsholtz, C. (1996). PDGF-A signaling is a critical event in lung alveolar myofibroblast development and alveogenesis. *Cell* **85,** 863-873.

Braun, T., Rudnicki, M. A., Arnold, H. H. and Jaenisch, R. (1992). Targeted inactivation of the muscle gene *Myf*-5 results in abnormal rib development and perinatal death. *Cell* **71,** 369-82.

Bronner-Fraser, M. (1995). Origins and developmental potential of the neural crest. *Exp. Cell Res.* **218,** 405-417.

Brunkow, M. E., Nagle, D. L., Bernstein, A. and Bucan, M. (1995). A 1.8-Mb YAC contig spanning three members of the receptor tyrosine kinase gene family (Pdgfra, Kit, and Flk1) on mouse chromosome 5. *Genomics* **25,** 421-432.

Candia, A. F., Hu, J., Crosby, J., Lalley, P. A., Noden, D., Nadeau, J. H. and Wright, C. V. (1992). Mox-1 and Mox-2 define a novel homeobox gene subfamily and are differentially expressed during early mesodermal patterning in mouse embryos. *Development* **116,** 1123-1136.

Chabot, B., Stephenson, D. A., Chapman, V. M., Besmer, P. and Bernstein, A. (1988). The proto-oncogene *c-kit* encoding a transmembrane tyrosine kinase receptor maps to the mouse W locus. *Nature* **335,** 88-89.

Claesson-Welsh, L. (1994). Platelet-derived growth factor receptor signals. *J. Biol. Chem.* **269,** 32023-32026.

Conlon, R. A., Reaume, A. G. and Rossant, J. (1995). *Notch1* is required for the coordinate segmentation of somites. *Development* **121,** 1533-1545.

Dickinson, M. E., Selleck, M. A. J., McMahon, A. P. and Bronner-Fraser, M. (1995). Dorsalization of the neural tube by the non-neural ectoderm. *Development* **121,** 2099-2106.

Duttlinger, R., Manova, K., Berrozpe, G., Chu, T.-Y., DeLeon, V., Timokhina, I., Chaganti, R. J. K., Zelenetz, A. D., Bachvarova, R. F. and Besmer, P. (1995). The *Wsh* and *Ph* mutations affect the *c-kit* expression profile: *c-kit* misexpression in embryogenesis impairs melanogenesis in *Wsh* and *Ph* mutant mice. *Proc. Natl. Acad. Sci. USA* **92,** 3754-3758.

Fan, C.-M. and Tessier-Lavigne, M. (1994). Patterning of mammalian somites by surface ectoderm and notochord: evidence for sclerotome induction by a hedgehog homolog. *Cell* **79,** 1175-1186.

Geissler, E. N., Ryan, M. A. and Housman, D. E. (1988). The dominant-White Spotting (W) locus of the mouse encodes the *c-kit* proto-oncogene. *Cell* **55,** 185-192.

Grass, S., Arnold, H.-H. and Braun, T. (1996). Alterations in somite patterning of *myf-5* deficient mice: a possible role for FGF-4 and FGF-6. *Development* **122,** 141-150.

Grüneberg, H. (1963). *The Pathology of Development.* Oxford: Blackwell Scientific Publications.

Grüneberg, H. and Truslove, G. M. (1960). Two closely linked genes in the mouse. *Genet. Res.* **1,** 69-90.

Helwig, U., Imai, K., Schmahl, W., Thomas, B. E., Varnum, D. S., Nadeau, J. H. and Balling, R. (1995). Interaction between undulated and Patch leads to an extreme form of spina bifida in double-mutant mice. *Nature Gen.* **11,** 60-63.

Hogan, B., Beddington, R., Costantini, F. and Lacy, E. (1994). *Manipulating the Mouse Embryo: a Laboratory Manual.* Cold Spring Harbor Laboratory,

Imamoto, A. and Soriano, P. (1993). Disruption of the *csk* gene, encoding a negative regulator of Src family tyrosine kinases, leads to neural tube defects and embryonic lethality in mice. *Cell* **73,** 1117-1124.

Jeffs, P., Jaques, K. and Osmond, M. (1992). Cell death in cranial neural crest development. *Anat. Embryol.* **185,** 583-588.

Jeffs, P. and Osmond, M. (1992). A segmented pattern of cell death during development of the chick embryo. *Anat. Embryol.* **185,** 589-598.

Kazlauskas, A. (1994). Receptor tyrosine kinases and their targets. *Curr. Opin. Genet. Dev.* **4,** 5-14.

Koyama, N., Morisaki, N., Saito, Y. and Yoshida, S. (1992). Regulatory effects of platelet-derived growth factor AA homodimer on migration of vascular smooth muscle cells. *J. Biol. Chem.* **267,** 22806-22812.

Le Douarin, N. M., Ziller, C. and Couly, G. F. (1993). Patterning of neural crest derivatives in the avian embryo: *in vivo* and *in vitro* studies. *Dev. Biology* **159,** 24-49.

Levéen, P., Pekny, M., Gebre-Medhin, S., Swolin, B., Larsson, E. and Betsholtz, C. (1994). Mice deficient for PDGF B show renal, cardiovascular, and hematological abnormalities. *Genes Dev.* **8,** 1875-1887.

Liem, K. F., Tremmi, G., Roelink, H. and Jessell, T. M. (1995). Dorsal differentiation of neural plate cells induced by BMP-mediated signals from epidermal ectoderm. *Cell* **82,** 969-979.

Morrison-Graham, K., Schatteman, G. C., Bork, T., Bowen-Pope, D. F. and Weston, J. A. (1992). A PDGF receptor mutation in the mouse (*Patch*) perturbs the development of a non-neuronal subset of neural crest-derived cells. *Development* **115,** 133-142.

Nagle, D. L., Martin-DeLeon, P., Hough, R. B. and Bucan, M. (1994). Structural analysis of chromosomal rearrangements associated with the developmental mutations *Ph*, *W19H*, and *Rw* on mouse chromosome 5. *Proc. Natl. Acad. Sci. USA* **91,** 7237-7241.

Olson, E. N., Arnold, H.-H., Rigby, P. W. J. and Wold, B. J. (1996). Know your neighbors: three phenotypes in null mutants of the myogenic bHLH gene *MRF4*. *Cell* **85,** 1-4.

Orr-Urtreger, A., Bedford, M. T., Do, M. S., Eisenbach, L. and Lonai, P. (1992). Developmental expression of the α receptor for platelet-derived growth factor, which is deleted in the embryonic lethal *Patch* mutation. *Development* **115,** 289-303.

Orr-Urtreger, A. and Lonai, P. (1992). Platelet-derived growth factor-A and

its receptor are expressed in separate, but adjacent cell layers of the mouse embryo. *Development* **115,** 1045-1058.

Payne, J., Shibasaki, F. and Mercola, M. (1997). Spina bifida occulta in homozygous Patch mouse embryos. *Developmental Dyn.* **209**, 105-116.

Raff, M. C. (1992). Social controls on cell survival and cell death. *Nature* **356,** 397-400.

Raff, M. C., Barres, B. A., Burne, J. F., Coles, H. S., Ishizaki, Y. and Jacobson, M. D. (1993). Programmed cell death and the control of cell survival: lessons from the nervous system. *Science* **262,** 695-700.

Ross, R., Raines, E. W. and Bowen-Pope, D. F. (1986). The biology of platelet-derived growth factor. *Cell* **46,** 155-169.

Schatteman, G. C., Morrison-Graham, K., van Koppen, A., Weston, J. A. and Bowen-Pope, D. F. (1992). Regulation and role of PDGF receptor α-subunit expression during embryogenesis. *Development* **115,** 123-131.

Seifert, R. A., Hart, C. E., Phillips, P. E., Forstrom, J. W., Ross, R., Murray, M. J. and Bowen-Pope, D. F. (1989). Two different subunits associate to create isoform-specific platelet-derived growth factor receptors. *J. Biol. Chem.* **264,** 8771-8778.

Selleck, M. A. and Bronner-Fraser, M. (1995). Origins of the avian neural crest: the role of neural plate-epidermal interactions. *Development* **121,** 525-538.

Smith, E. A., Seldin, M. F., Martinez, L., Watson, M. L., Choudhury, G. G., Lalley, P. A., Pierce, J., Aaronson, S., Barker, J., Naylor, S. L. and Sakaguchi, A. Y. (1991). Mouse platelet-derived growth factor receptor α gene is deleted in W19H and patch mutations on chromosome 5. *Proc. Natl. Acad. Sci. USA* **88,** 4811-4815.

Soriano, P. (1994). Abnormal kidney development and hematological disorders in PDGF β-receptor mutant mice. *Genes Dev.* **8,** 1888-1896.

Soriano, P., Montogomery, C., Geske, R. and Bradley, A. (1991). Targeted disruption of the c-*src* proto-oncogene leads to ospeopetrosis in mice. *Cell* **64,** 693-702.

Spence, M. S., Yip, J. and Erickson, C. A. (1996). The dorsal neural tube organizes the dermomyotome and induces axial myocytes in the avian embryo. *Development* **122,** 231-241.

Stephenson, D. A., Mercola, M., Anderson, E., Wang, C., Stiles, C. D., Bowen-Pope, D. F. and Chapman, V. M. (1991). Platelet-derived growth factor receptor α-subunit gene (*Pdgfra*) is deleted in the mouse patch (*Ph*) mutation. *Proc. Natl. Acad. Sci. USA* **88,** 6-10.

Symes, K. and Mercola, M. (1996). Embryonic mesoderm cells spread in response to platelet-derived growth factor and signaling by phosphatidylinositol 3-kinase. *Proc. Natl. Acad. Sci. USA* **93,** 9641-9644.

Truslove, G. M. (1977). A new allele at the patch locus in the mouse. *Genet. Res.* **29,** 183-186.

Wang, C. and Stiles, C. D. (1994). Platelet-derived growth factor α receptor gene expression: isolation and characterization of the promoter and upstream regulatory elements. *Proc. Natl. Acad. Sci. USA* **91,** 7061-7065.

Wehrle-Haller, B., Morrison-Graham, K. and Weston, J. A. (1996). Ectopic c-kit expression affects the fate of melanocyte precursors in Patch mutant embryos. *Dev. Biol.* **177,** 463-474.

Yu, J.-C., Mahadevan, D., LaRochelle, W. J., Pierce, J. H. and Heidaran, M. A. (1994). Structural coincidence of αPDGFR epitopes binding to platelet-derived growth factor AA and a potent neutralizing monoclonal antibody. *J. Biol. Chem.* **269,** 10668-10674.

(Accepted 9 May 1997)